Nature Environment and Pollution Technology
An International Quarterly Scientific Journal

ISSN: 0972-6268	Vol. 13	No. 1	pp. 95-99	2014

Original Research Paper

Study on Spatial Migration Law of Heavy Metal Copper in Soil-*Ligustrum lucidum* Plant Interface System

Jin Xiang Yang, Xiao Long Li, Liangmin Gao, Duoxi Yao and Ming Xu Zhang
The School of Earth and Environmental Science, Anhui University of Science and Technology, Huainan, Anhui, China

Nat. Env. & Poll. Tech.
Website: www.neptjournal.com
Received: 24-12-2013
Accepted: 26-1-2014

Key Words:
Migration law
Copper
Soil-root interface
Ligustrum lucidum

ABSTRACT

Spatial distribution characteristics of heavy metals in soil-root system have important significance for the research of soil pollution risk assessment and phytoremediation effect. Taking *Ligustrum lucidum* plant as an example in this paper, according to the characteristics of adsorption of heavy metals in soil by woody plants, laying out sampling points, using Sufer software for Kiging interpolation analysis, horizontal migration law of heavy metal copper in the soil-root interface system was simulated. Through multi-model statistical regression trend analysis, the horizontal migration mechanism of copper in different section has been discussed. The results showed that under horizontal migration law in the surface soil, the migration capability of Cu by root in soil near the roots is relatively weak; with root extending, the migration capability is strengthened gradually. In the deeper soil, the migration law with the root extension was gradually weaker, and the main range of accumulation ability is 60-90cm in three sections. In addition, its migration law follows the cubic curve mode. Under longitudinal migration law, based on the Kriging method, migration models $Z(hi)$ of heavy metal Cu in any depth of h_i are constructed.

INTRODUCTION

During growth and development of plant, root and root hair interspersed in all the space of root layer soil, and could selectively absorb some heavy metal ions in soil solution. Plants adsorbed heavy metal ions to cause increase of their concentration in root soil solution, and form gradually increased solute potential distribution in soil-root. Therefore, as a result of plant root absorption and evaporation effect, heavy metal ions could form a certain special distribution law in soil-root interface system. Making use of four kinds of Kriging methods, the spatial distribution of soil Pb in the soil was estimated (Cattle et al. 2002). Spatial variability of heavy metals was compared in the study area (Paz-Gonzalez et al. 2002). The heavy metals content in soil was estimated using Kriging method, which improved the estimation accuracy (Goovaerts et al. 1997, Jiang et al. 2004). Taking Huainan reclamation area in China as an example, according to the characteristics of adsorption of heavy metals in soil by woody plants, using different methods, the special migration law of heavy metal copper in soil-woody plants root interface was discussed in this paper, which provided the coal mine woody plants reclamation of heavy metal pollution in coal mine reclamation area for scientific basis.

MATERIALS AND METHODS

Sample collection: According to the land reclamation of Huainan mining area, as well as the restored vegetation condition and research content, taking ligustrum lucidum as an example, the spatial migration law of copper was discussed in soil-root interface.

Sampling layout scheme: According to distribution range of ligustrum lucidum root, three radiations (W, S, N) were laid out in the horizontal direction; five sampling points were laid out in each radiation. The layout requirements of each sampling point are listed in Table 1. In the vertical direction, because filling thickness of coal gangue was about 60cm, each sampling point in a vertical was set in four sections, namely 0, 20cm, 40cm and 60cm. The specific distribution is shown in Fig. 1.

Pretreatment and test of samples: Soil samples in strict accordance with the soil environmental monitor technical specification (HJ/T 166-2004) were treated. The soil samples were put in a ventilated, cool and dry place to naturally air dry. After drying, the stones, plant roots and other debris were picked out from the samples, and then according to quartering, the samples were discarded the excess part to retain about 300 g or so. Finally the samples were put in agate mortar for grinding, passed through 18, 100 and 200 eye nylon screen mesh for screening, and sealed into ziplock bag to prepare for determination.

The samples were accurately weighted 0.5 g to digest with HCl-HNO_3-HF-$HClO_4$, and use of HNO_3 (0.2%) for constant volume 50 mL. They were tested using graphite furnace method by using the instrument TAS-986 type

Table 1: Sampling layout scheme; Unit: cm

Points	W0	W1	W2	W3	W4	N0	S1	S2	S3	S4	N0	N1	N2	N3	N4
Distance from origin	15	30	60	90	120	15	30	60	90	120	15	30	60	90	120

Note: Taking *Ligustrum lucidum* as the origin.

Table 2: Coordinate position of sampling points.

Sampling Points	W0	W1	W2	W3	W4
Coordinate	(15, 0)	(30, 0)	(60, 0)	(90, 0)	(120, 0)
Sampling points	S0	S1	S2	S3	S4
Coordinate	(-6.34,-13.59)	(-12.68,-27.19)	(-25.36,-54.38)	(-38.04,-81.57)	(-50.71,-108.76)
Sampling points	N0	N1	N2	N3	N4
Coordinate	(-4.88,14.18)	(-9.77,28.37)	(-19.53,56.73)	(-29.30,85.10)	(-39.07,113.46)

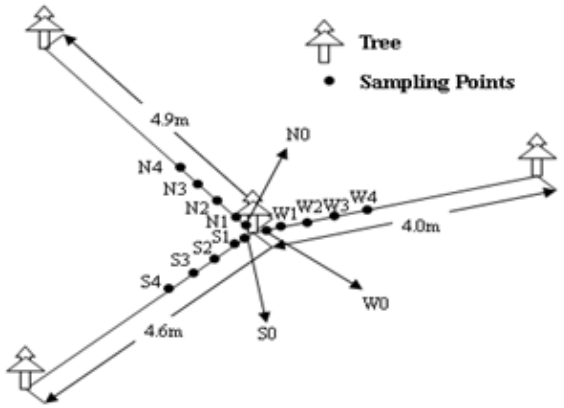

Fig. 1: Sampling points layout scheme.

atomic absorption spectrophotometer.

RESULTS AND DISCUSSION

Horizontal migration law of copper in soil-root interface system: According to the trigonometric function of each radiation, taking ligustrum lucidum as the origin O, and W radiation line as X axis, coordinate system was established. The specific coordinate position of each sampling point is shown in Table 2. Using Kriging interpolation analysis of Surfer software, the migration law of copper in soil-root interface system was simulated. Taking use of Excel and Spss software for multiple model regression trend analysis, the horizontal migration mechanism of copper in different sections in soil-root system was discussed. The results are shown in Fig. 2.

Near the root, namely 0-30cm range, the roots grow downward and accumulation capability of Cu by root in soil near the roots is relatively weak, so that its content is relatively low, that is migration ability of Cu is weaker. With root extending, accumulation capability is strengthened, and the content of Cu increases gradually reaching the peak at about 90cm, followed by decrease, that is migration ability of Cu is stronger within 60-90cm in the surface soil. In the 20-40cm and 40-60cm sections, migration law of Cu has better consistency. The accumulation ability of Cu near the root is stronger because of developed root, and that is migration ability is greater; with the root extension, the accumulation capability was gradually weaker, so the main range of accumulation capacity is 30-90cm. From the migration law of Cu in the three sections, the main range of accumulation capacity is 60-90cm. Through the multiple model regression trend analysis of Spss, the result is that in numerous model regression, the fitting effect of cubic curve model is optimal, that is migration law of copper in soil-ligustrum lucidum root interface system followed cubic curve model, the fitting effect of R^2 is greater than 0.712.

Longitudinal migration law of copper in soil-root interface system: According to sampling survey in reclamation area soil, the spatial distribution of heavy metal Cu content was analysed in soil-root interface system using the Kriging method to explore migration mechanism of the heavy metal Cu. According to the research results on the festival, ligustrum lucidum had strong absorption and enrichment capacity for Cu in soil-root interface system, and the main range of its accumulation capacity was 60-90cm. Therefore, when the Kriging model was established, it was necessary to consider the migration characteristics of Cu according to the segmental distance, namely 0-30cm, 60-90cm and > 120cm.

***Construction of semi-variation function mathematical model*:** According to Kriging method, at first semi-variation function of the n known samples corresponding to the $z(h_i)$ in different depths (h) should be constructed, and then semi-variation function $r(h)$ value of the different h was calculated. Secondly, taking h as abscissa and $r(h)$ as the ordinate, the scatter diagram was made, and the use of the proper

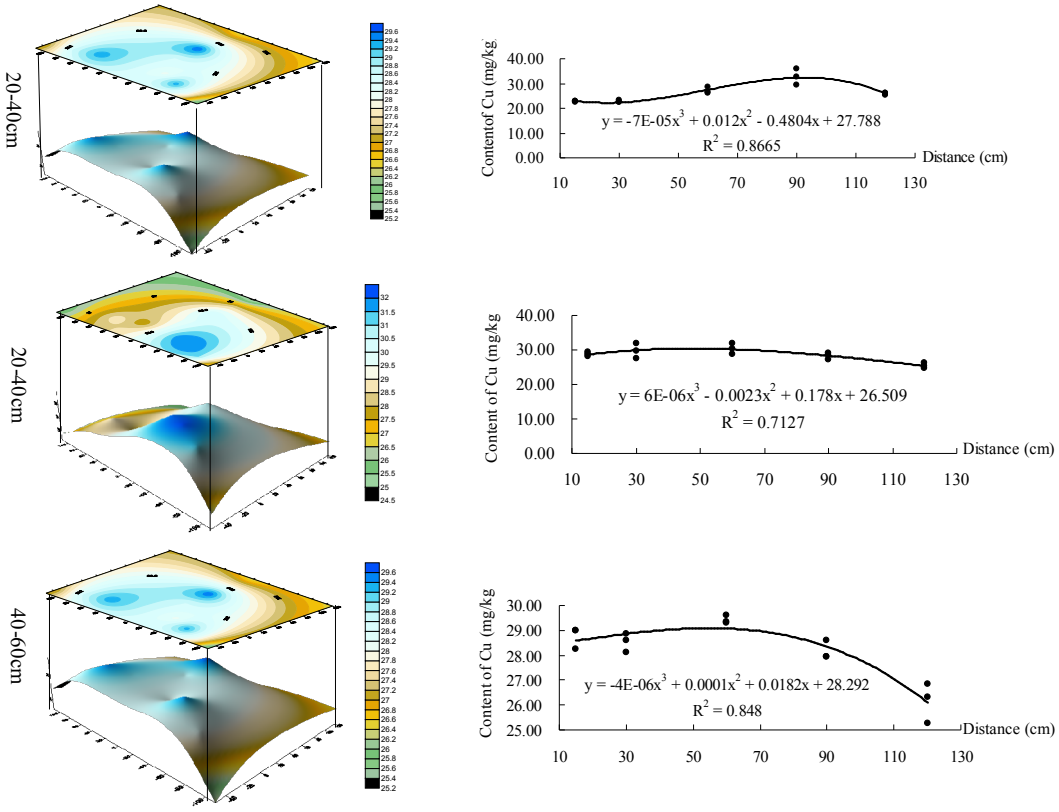

Fig. 2: Migration law of copper in soil-root interface system.

function was used to fit (using linear function to fit in this paper). So that the expression of $r(h)$ was obtained (Hu et al. 2006, Jiang et al. 2004).

$$r(h) = \frac{1}{2m_{|h_i - h_j = h|}} \sum \left(z(h_i) - z(h_j)\right)^2 \quad ...(1)$$

Where, h_i (i = 1, 2,..., n) was n sampling points; $z(h_i)$ was the content value of heavy metal Cu in h_i depth place; h was the distance between h_i and h_j or $|h_i - h_j| = h$; the distance which was h had m pairs during n sampling points (Dong et al. 2010).

The semi-variation functions of the sampling points were respectively solved using the formula (1), and the results are given in Table 3.

The groups having the relative volatility of value larger were removed, and then the mean values were calculated (Table 5).

Taking use of the results in Table 4, the scatter diagram was made (Fig. 3).

***Constructing matrix W*:** According to the above results, the matrix W was constructed. In order to record convenience, the matrix W was recorded in the form of Table (Table 5).

***Constructing matrix Y*:** Using the measured sample values, the heavy metal content matrix Y was built. Because the same depth had several samples, when matrix Y was constructed, the values of rest sample points at the corresponding depth were taken mean after get rid of (1), namely:

$$Y_{Cu(0\text{-}30)} = |\,21.4903\ 22.8736\ 28.5762\ \ 28.6104\ 0\,|$$

$$Y_{Cu(60\text{-}90)} = |\,25.9492\ 27.5714\ 30.5779\ \ 29.4080\ 0\,|$$

$$Y_{Cu(120)} = |\,24.6530\ 25.61825\ 25.8216\ \ 26.0571\ 0\,|$$

***Constructing matrix B*:** Taking use of semi-variation function value, matrix B was constructed. The corresponding h in different depths was different (h>0), therefore, it was necessary to consider according to the segmental depth h:

1. When 0<h ≤ 20 cm

0-30cm:

$B^T = |\,0.434h + 0.815, -0.434h + 9.501, -0.434h + 18.187, -0.434h + 26.873, 1|$

60-90cm:

$B^T = |\,0.0767h + 1.538, -0.0767h + 3.07, -0.0767h + 4.602, -0.0767h + 6.134, 1|$

Table 3: Semi-variation function value.

Points	r(20)	r(40)	r(60)
S0	7.3465	23.5899	25.2768
S1	17.0537	38.6895	27.7833
W0	6.9356	24.2183	28.8846
W1	7.4835	22.2704	22.1079
N0	3.7850	14.3906	18.6905
N1	4.3847	15.0725	17.4812
S2	3.7021	6.9791	3.2513
S3	2.2268	2.4312	0.0173
W2	3.4633	9.9301	9.4713
W3	10.5586	39.0012	48.4807
N2	1.0950	4.4024	6.0343
N3	4.8560	9.3518	5.7749
S4	0.4390	0.8845	0.4525
W4	1.8938	3.9950	2.5500
N4	0.5272	0.2492	1.7240

Table 4: r(h) value of Cu.

Range	r(20)	r(40)	r(60)
0-30cm	8.6408	19.9083	26.0131
60-90cm	3.0686	4.6042	6.1330
120cm	0.4831	0.5669	1.0883

Table 5: Matrix W.

Range	Matrix W				
0-30cm	0	8.6408	19.9083	26.0131	1
	8.6408	0	8.6408	19.9083	1
	19.9083	8.6408	0	8.6408	1
	26.0131	19.9083	8.6408	0	1
	1	1	1	1	1
60-90cm	0	3.0686	4.6042	6.1330	1
	3.0686	0	3.0686	4.6042	1
	4.6042	3.0686	0	3.0686	1
	6.1330	4.6042	3.0686	0	1
	1	1	1	1	1
120cm	0	0.4831	0.5669	1.0883	1
	0.4831	0	0.4831	0.5669	1
	0.5669	0.4831	0	0.4831	1
	1.0883	0.5669	0.4831	0	1
	1	1	1	1	1

> 120cm:

$B^T = |0.015h + 0.108, -0.015h + 0.410, -0.015h + 0.712, -0.015h + 0.410, 1|$

2. When 20 cm<x≤40 cm

0-30cm:

$B^T = |0.434h + 0.815, 0.434h - 7.871, -0.434h + 18.187, -0.434h + 26.873, 1|$

60-90cm:

$B^T = |0.0767h + 1.538, 0.0767h + 0.006, -0.0767h + 4.602, -0.0767h + 6.134, 1|$

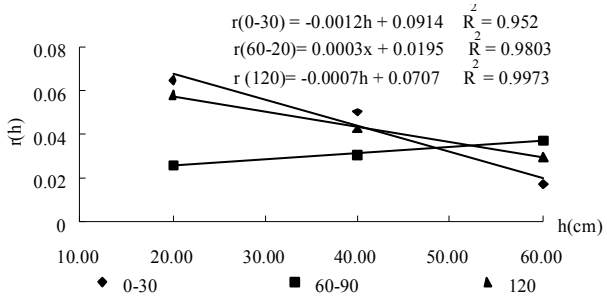

Fig. 3: Scatter diagram of semi-variation function.

According to the above scatter diagram, fitting out of r(h) expression for: 0-30cm; r(h) = -0.0012h + 0.0914, fitting correlation coefficient: $R^2 = 0.952$; 60-90cm; r(h) = 0.0003h + 0.0195, fitting correlation coefficient: $R^2 = 0.980$; 120cm; r (h) = -0.0007h + 0.0707, fitting correlation coefficient: $R^2 = 0.9970$

> 120cm:

$B^T = |0.015h + 0.108, 0.015h - 0.194, -0.015h + 0.712, -0.015h + 0.410, 1|$

3. When 40 cm<x ≤ 60 cm

0-30cm:

$B^T = |0.434h + 0.815, 0.434h - 7.871, 0.434h - 16.557, -0.434h + 26.873, 1|$

60-90cm:

$B^T = |0.0767h + 1.5376, 0.0767h + 0.006, 0.0767h - 1.526, -0.0767h + 6.134, 1|$

> 120cm:

$B^T = |0.015h + 0.108, 0.015h - 0.194, 0.015h - 0.496, -0.015h + 0.410, 1|$

***Function model $Z(h_i)$ of heavy Cu in any depth h_i*:** By Kriging method, estimated value of heavy metal Cu at any point h_i was $Z(h_i) = Y^T W^{-1} B$ (Meul et al. 2003), function model $Z(h_i)$ of heavy metal Cu in any depth h_i could be calculated. The results were as follows:

1. When 0<h≤20 cm

Function model $Z(h_i)$ of Cu:

0-30cm: $Z(h_i) = -0.087h + 23.902$

60-90cm: $Z(h_i) = -0.176h + 33.733$

120cm: $Z(h_i) = -0.021h + 41.878$

2. When 20 cm<x≤40 cm

Function model $Z(h_i)$ of Cu:

0-30 cm: $Z(h_i) = 0.290h + 16.345$

60-90 cm: $Z(h_i) = 0.089h + 28.444$

120 cm: $Z(h_i) = 0.022h + 41.015$

3. When 40 cm<x≤60 cm

Function model $Z(h_i)$ of Cu:

0-30 cm: $Z(h_i) = 0.063h + 25.428$

60-90 cm: $Z(h_i) = 0.232h + 22.754$

120 cm: $Z(h_i) = 0.059h + 39.531$

CONCLUSIONS

Through the above study and analysis, the following conclusions were drawn:

1. Horizontal migration mechanism of copper in soil-root interface system: In the surface soil, the migration capability of Cu by root in soil near the roots is relatively weak; with root extending, the migration capability is strengthened gradually, and reaches a peak at about 90cm, and then decreases. In the deep soil, the migration law of Cu with the root extension was gradually weaker. From migration law of Cu in the three sections, the main range of accumulation capacity is 60-90cm. And migration law of copper in soil-ligustrum lucidum root interface system follows cubic curve mode.
2. Longitudinal migration mechanism of Cu in soil-root interface system: According to the Kriging method, migration models Z(hi) of heavy metal Cu in any depth h_i were constructed, and fitting correlation coefficient is greater. In practical application, at the different distances from root in the range of different profiles, there are the corresponding fitting equations; the content of copper on non-sampling layer is calculated through the equation, which compensates for the defects that longitudinal profile sampling interval of large, and implements research of spatial distribution of heavy metal copper in soil from qualitative description to quantitative calculation.

ACKNOWLEDGEMENT

This work was financially supported by the provincial outstanding young talent fund project in 2012 (2012SQRL054)

REFERENCES

Andronikov, S.V., Davidson, D.A. and Spiers, R.B. 2000. Variability in contamination by heavy metals: Sampling implication. Water Air Soil Poll., 120(1): 29-45.

Cahoon, L.B. and Ensign, S.H. 2004. Spatial and temporal variability in excessive soil phosphorus levels in Eastern North Carolina. Nutr. Cycl. Agroecosyst, 69(2): 111-125.

Cattle, J.A., McBrantney, A.B. and Minasny, B. 2002. Kriging method evaluation for assessing the spatial distribution of urban soil lead contamination. Journal of Environmental Quality, 31: 1576-158

Chen, F. S., Zeng, D. H. and Chen, G. S. 2004. Effect of land use change on spatial distribution pattern of soil total nitrogen in Keerqin sandy land. Chin. J. Appl. Ecol., 15(6): 953-95.

Dong, J. H., Bian, Z. F., Yu, M. and Di, L. 2010. Distribution of heavy metals in reclamation soils of mining area. Journal of China University of Mining & Technology, 39(3): 335-341.

Goovaerts, P., Webster, R. and Dubois, J.P. 1997. Assessing the risk of soil contamination in the Swiss Jura using indicator geostatistics. Environmental and Ecological Statistics, 4: 31-48.

Guo, X.D., Fu, B.J., Ma, K.M., Chen, L.D. and Yang, F.L. 2000. Spatial variability of soil nutrients based on geostatistics combined with GIS - A case study in Zunhua City of Hebei Province. Chin. J. Appl. Ecol., 11(4): 557-563.

Hu, K.L., Zhang, F.R., Lu, Y.Z., Wang, R. and Xu, Y. 2004. Spatial distribution of concentrations of soil heavy metals in Daxing County, Beijing. Acta Sci. Circ., 24(3): 463-468.

Jiang, Y., Li, Q., Zhang, X.K. and Liang, W.J. 2006. Kinging prediction of soil zinc in contaminated field by using an auxiliary variable. Chinese Journal Applied Ecology, 17(10): 97-101.

Jiang, K., Chen, Y. and Li, D. 2004. Using sequential indicator simulation to assess the uncertainty of delineating heavy-metal contaminated soils. Environmental Pollution, 127: 229-238.

Lark, R.M. and Ferguson, R.B. 2004. Mapping risk of soil nutrient deficiency or excess by disjuctive and indicator Kriging. Geoderma, 118(1): 39-53.

Liang, W.J., Li, Q., Jiang, Y. and Zhang, X.K. 2003. The effect of cultivation on the spatial distribution of nematode trophic groups in black soil. Pedosphere, 13(2): 97-102.

Meul, M. and Van Meirvenne, M. 2003. Kriging soil texture under different types of nonstationarity. Geoderma, 112(3): 217-233.

Paz-Gonzalez, A., Castro, M. T. T. and Vieira, S. R. 2002. Geostatistical analysis of heavy metal in a one hectare plot under natural vegetation in a serpentine area. Canadian Journal of Soil Science, 81(3): 469-479.

White, J.G., Welch, R.M. and Norvell, W.A. 1997. Soil zinc map of the USA using geostatistics and geographic information systems. Soil Sci. Soc. Am. J., 61(1): 185-194.

Yang, M., Liu, H.B. and Wu, W. 2006. Spatial variability of heavy metals in soil of Three-Gorges Reservoir in Chongqing. Chinese Journal of Eco-Agriculture, 14(1): 100-103.

Yang, J. X. and Zhang, M. X. 2011. Migration law of heavy metals in coal gangue. Advances in Intelligent and Soft Computing, 106.

Zhang, Z.G., Yao, D.X. and Zheng, Y.H. 2010. The phytoremediation potential of six Compositae plants to soil pollution of heavy metal in coal mine collapse and reclaimed area. Journal of China Coal Society, 35(10): 1742-1747.